Electron transport in W-containing amorphous carbon–silicon diamond-like nanocomposites

2004 J. Phys.: Condens. Matter 16 8447

(http://iopscience.iop.org/0953-8984/16/46/029)

INSTITUTE OF PHYSICS PUBLISHING JOURNAL OF PHYSICS: CONDENSED MATTER

J. Phys.: Condens. Matter **16** (2004) 8447–8458 PII: S0953-8984(04)76367-5

Electron transport in W-containing amorphous carbon–silicon diamond-like nanocomposites

A Bozhko[1], T Takagi[2,4], T Takeno[2] and M Shupegin[3]

[1] Physics Department, Moscow State University, Moscow 119899, Russia
[2] Institute of Fluid Science, Tohoku University, Sendai 980-8577, Japan
[3] Moscow Power Engineering Institute, Moscow 105835, Russia

E-mail: t.takagi@ieee.org

Received 16 February 2004
Published 5 November 2004
Online at stacks.iop.org/JPhysCM/16/8447
doi:10.1088/0953-8984/16/46/029

Abstract

The electron transport in amorphous hydrogenated carbon–silicon diamond-like nanocomposite films containing tungsten over the concentration range 12–40 at.% was studied in the temperature range 80–400 K. The films were deposited onto polycrystalline substrates, placed on the RF-biased substrate holder, by the combination of two methods: PECVD of siloxane vapours in the stimulated dc discharge and dc magnetron sputtering of tungsten target. The experimental dependences of the conductivity on the temperature are well fitted by the power-law dependences over the entire temperature range. The results obtained are discussed in terms of the model of inelastic tunnelling of the electrons in amorphous dielectrics. The average number of localized states $\langle n \rangle$ in the conducting channels between metal clusters calculated in the framework of this model is characterized by the non-monotonic dependence on the tungsten concentration in the films. The qualitative explanation of the results on the basis of host carbon–silicon matrix structural modifications is proposed. The evolution of the carbon–silicon matrix microstructure by the increase in the tungsten concentration is confirmed by the Raman spectroscopy data.

1. Introduction

Hard amorphous carbon coatings continue to attract attention due to their interesting, and often unusual properties over the last two decades. The diamond-like carbon films, which belong to this class of materials, are related to perfect insulators whose conductivity is dependent on deposition conditions [1]. In [2–6], it was shown that the addition of different metals to the hydrogenated carbon films during deposition enhances their conductivity over many orders of magnitude up to the values typical for the amorphous metals. The metal phase exists in the

[4] Author to whom correspondence should be addressed.

films in the form of nanometer-sized metal particles or nanoclusters dispersed in an insulating carbon host matrix.

The dependence of the conductivity on metal concentration in metal–carbon nanocomposites has the features of universality typical for the metal–insulator mixtures and is described by the percolation theory [7]. Far enough in the metallic region, the character of the conductivity is close to that of amorphous metals. On the other hand, when the concentration of the metal is less than the critical value x_c, the carbon–metal nanocomposites can be considered as amorphous dielectrics.

The charge transfer mechanisms in metal–insulator mixtures are usually discussed in terms of the electron tunnelling between metal particles. The influence of the insulating host matrix microstructure on the tunnelling processes should also be taken into account. Especially, this is true in the case of carbon and carbon-containing matrices, where the high fluctuations of the random potential take place due to the coexistence of the different types of carbon bonds.

The aim of this paper is to study the effect of tungsten concentration on the charge transport character in the hydrogenated amorphous carbon–silicon nanocomposite films containing tungsten.

Understanding the nature of the conductivity in these films will be of interest not only from the point of view as a possible charge-transport mechanism in highly disordered metal–carbon systems. The possible industrial applications of the investigated amorphous metal-containing carbon–silicon nanocomposite films, e.g. as advanced temperature sensors, which can combine the attractive properties typical for the traditional hard amorphous carbon coatings with a new functionality imparted by the presence of metal nanoclusters in highly disordered carbon-based matrix may also be considered.

2. Experimental details

The films of W-containing amorphous carbon–silicon nanocomposites were grown on the polycrystalline substrates by the two combined processes: stimulated dc discharge (plasma current 1–4 A, voltage 150 V) of siloxane ($(CH3)_3SiO(CH_3C_6H_5SiO)_3Si(CH_3)_3$) vapours and dc magnetron sputtering of W target. The RF (1.76 MHz) bias voltage (0–5 kV) was applied to the substrate holder during deposition.

The properties of the deposited films of hydrogenated amorphous carbon–silicon nanocomposites, for a very low concentration of the metal, approach those typical for the conventional diamond-like films [8]. The concentration of silicon and oxygen in pure carbon–silicon matrix is in the range 10–20 at.%, being dependent on the value of tungsten concentration.

A detailed description of the deposition method and structural properties of the films studied in the present paper can be found elsewhere [8, 9].

The samples for the conductivity measurements were prepared in a standard 4-probe geometry fabricated by argon plasma etching using a mechanical mask. The contacts to the samples were prepared using silver paint. In order to decrease the resistance of the contacts and to increase their stability, an additional Au sublayer was predeposited on the area of the contacts on the samples through a mechanical mask.

The conductivity was measured in a gas flow cryostat by the standard low-frequency ac lock-in technique.

The tungsten concentration in the films was studied by an Electron Probe Micro Analyzer JEOL JXA-8200. The concentration measurements were performed in the region between the potential contacts in order to decrease the effect of large-scale concentration inhomogeneities on the measurements.

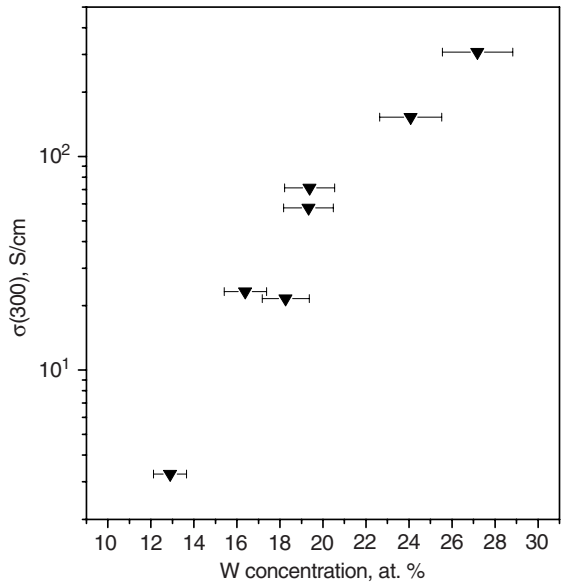

Figure 1. Room temperature conductivity as a function of tungsten concentration in W-containing amorphous carbon–silicon nanocomposite films.

Evaluation of the effect of tungsten concentration on the carbon phase structure over the entire W concentration range was performed by the Raman spectrometer Jobin Yvon LabRAM HR-800, using the 632.8 nm line of He–Ne laser in the range 800–1800 cm^{-1} with 20 mW power.

3. Results and discussion

In figure 1, the dependence of room temperature ($T = 300$ k) conductivity σ (300) on tungsten concentration varied over the range 12–30 at.% is presented on a log–log scale. In this concentration range, conductivity changes by approximately two orders of magnitude—from 3 to 300 $(\Omega\,cm)^{-1}$.

Figure 2 shows the dependence of the normalized conductivity $\sigma(T)/\sigma(300)$ of the tungsten-containing amorphous carbon–silicon nanocomposite films on the temperature. This representation of the conductivity data was chosen in order to show the fine structure of wide-ranged experimental curves placed in one figure. The solid lines in figure 2 are the results of the fitting procedure discussed below. One can see that the conductivity of all the samples studied decreases monotonically with decrease in temperature. The value of total variation of the conductivity in the investigated temperature range, defined as $(\sigma(380) - \sigma(80))/\sigma(300)$, increases with decrease in tungsten concentration. Moreover, the curvature of $\sigma(T)$ dependence changes its sign when the value of tungsten concentration exceeds 16–17 at.%.

The Raman spectra of metal–carbon nanocomposite films taken over the range 800–1800 cm^{-1} with linearly subtracted background are shown in figure 3. The number near each curve corresponds to the value of tungsten concentration in the films. The Raman spectra have a form typical for the amorphous hydrogenated a-C:H films. They are characterized by the existence of one broad non-symmetrical peak. The amplitude and shape of the peak are

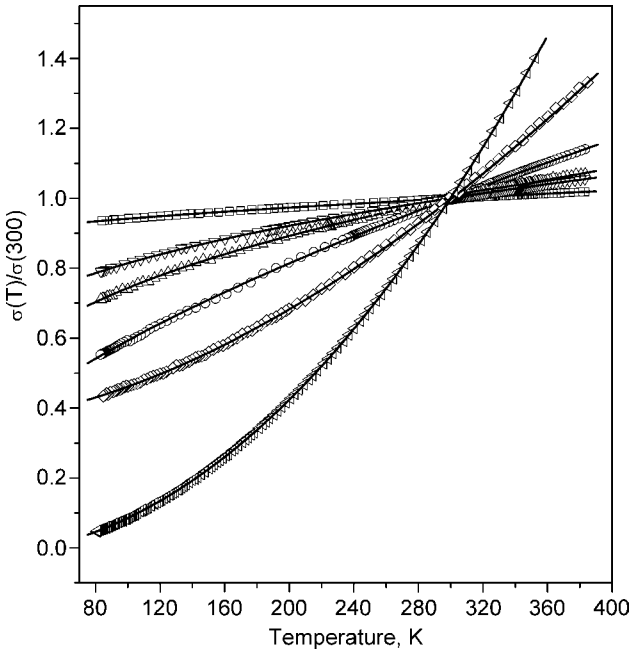

Figure 2. Dependence of the normalized conductivity $\sigma(T)/\sigma(300)$ on the temperature for the amorphous carbon–silicon nanocomposite films containing W. Concentration of W (in at.%): □, 38.5; ▽, 25.5; △, 18.8; ○, 17.5; ◇, 15.0; ◁, 13.5. The solid lines represent the best fitting following expression (2). The dependence of fitting parameters on W concentration is shown in figure 5 and is discussed in text.

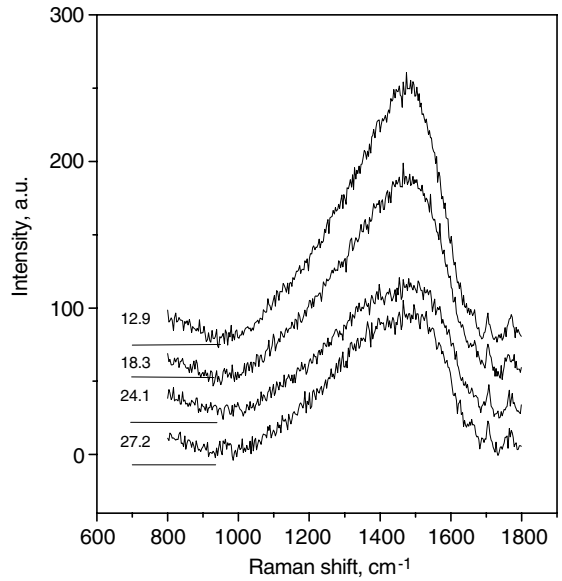

Figure 3. Typical Raman spectra of W-containing amorphous carbon–silicon nanocomposite films with subtracted linear background. The value of W concentration is shown near each curve. The curves are shifted for clarity. The short horizontal line near each curve shows the zero line.

very sensitive to the value of tungsten concentration. It can be deconvoluted at two Gaussian peaks. After fitting, one obtains the so-called D peak positioned at 1300–1400 cm^{-1} and G peak positioned at 1500–1600 cm^{-1}, respectively. In amorphous carbon, the G peak is ascribed to E_{2g} stretching vibrations of sp^2 pairs, while the D peak is associated with the A_{1g} breathing mode of the six-fold rings [21]. To the parameters, which are important for the characterization of carbon phase structure, the position of the G peak and the ratio of D- and G-peak intensities $I(D)/I(G)$ are related [22]. Figure 4 shows the evolution of these parameters in tungsten-containing amorphous carbon–silicon nanocomposite films on increase in the W concentration.

In the range of metal concentration below the metal–insulator transition, the electron transport in metal–dielectric nanocomposites occurs due to the thermally activated tunnelling of electrons between metal grains influenced by disorder, originated from the distribution of grain sizes and intergrain distances. The temperature dependence of the conductivity has an exponential character and follows the expression

$$\sigma \sim \exp\left[-\left(\frac{T_0}{T}\right)^m\right], \tag{1}$$

where T_0 is a characteristic temperature and m is an exponent, $m < 1$.

Experiments performed on a wide variety of metal–dielectric nanocomposites have shown that the conductivity in the wide temperature range usually follows (1) with m close to $1/2$. Various models were proposed for the explanation of this fact.

The nearest-neighbour hopping between metal grains in the presence of correlation between the metal grain diameter D and intergrain distance l: $l/D = \text{const}$ [10] or the less restrictive condition $\partial l/\partial D = \text{const}$ [11] leads to $m = 1/2$. The same value of m was observed in [12] for the Cu-containing SiO_2 films in the range of Cu concentration 17–33 vol.%, where the Coulomb interaction between the charged metal grains in the presence of a rather large random potential, which brings about the charge exchange between the initially neutral grains, in insulating SiO_2 matrix was assumed.

For an increase in metal concentration, metal–insulator transition takes place. Close to and on the metallic side, where the infinite conducting cluster composed of connected metal grains is formed, conductivity follows the power-law dependence on temperature:

$$\sigma = \sigma_0 + aT^p, \tag{2}$$

where σ_0 is the zero-temperature conductivity, positive on the metallic side of the transition, a is the prefactor and p is an exponent.

The value of power exponent p, determined by the electron transport mechanism, is dependent on the proximity of metal concentration to the metal–insulator transition point, temperature and magnetic field. In the vicinity of the metal–insulator transition, where the electron–electron interaction dominates, p takes values close to $1/3$, as it was observed in a number of papers, e.g., in [13] for V_xSi_{1-x} alloys for a value of V concentration close to 13 at.%.

On the metallic side of the metal–insulator transition, with increase in metal concentration the influence of the scattering of electrons on static defects increases that leads to $p = 1/2$. This fact was also reported in many papers, e.g. in the films of Pd_xC_{1-x} in the range of Pd concentration 30–34 vol.% [14] and V_xSi_{1-x} at V concentration exceeding 15 at.% [13].

The linear dependence of conductivity on temperature ($p = 1$) was observed in amorphous Cd–Sb alloys [20]. The results were discussed in terms of inelastic scattering of electrons at the structural disorder of the material.

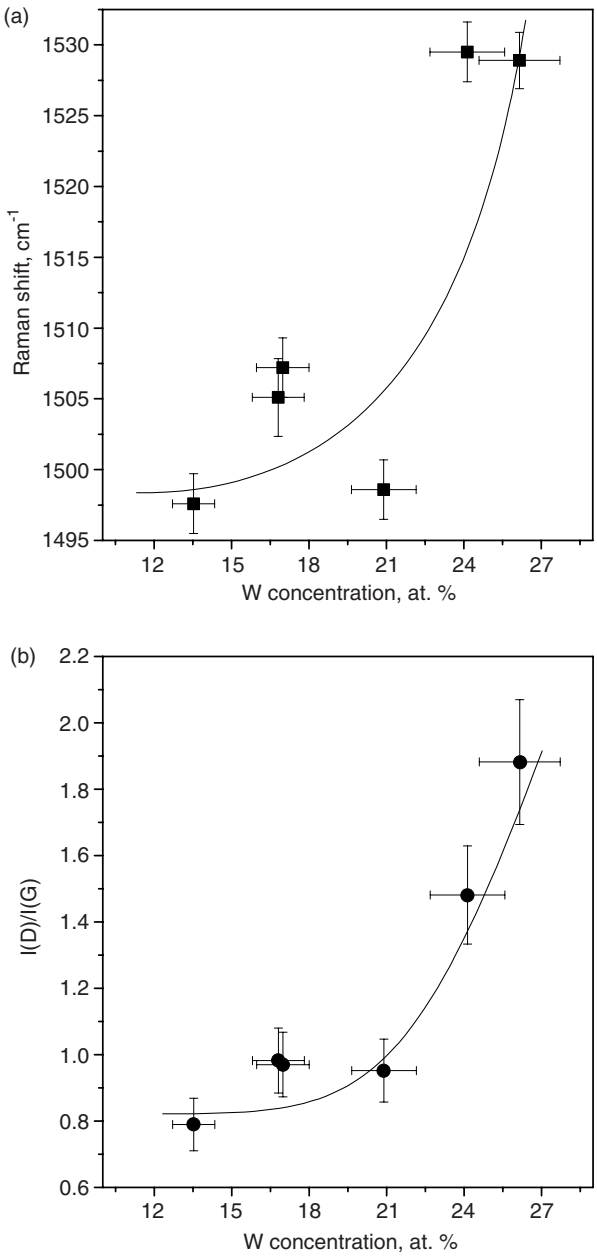

Figure 4. G peak position (a) and $I(\mathrm{D})/I(\mathrm{G})$ ratio (b) versus tugsten concentration of W-containing amorphous carbon–silicon nanocomposite films. Lines are guides to the eyes.

However, the power-law dependence of the conductivity can be observed also on the dielectric side of the metal–insulator transition. By the extension of the Coulomb charging model based on the assumption that at high temperature the multiply-ionized metal grains can play a dominant role in the conductivity, it was observed that at relatively high temperatures the dependence of the conductivity on the temperature was close to linear [18]. In the same paper, the data from [19] were analysed in terms of the proposed model and a reasonable agreement

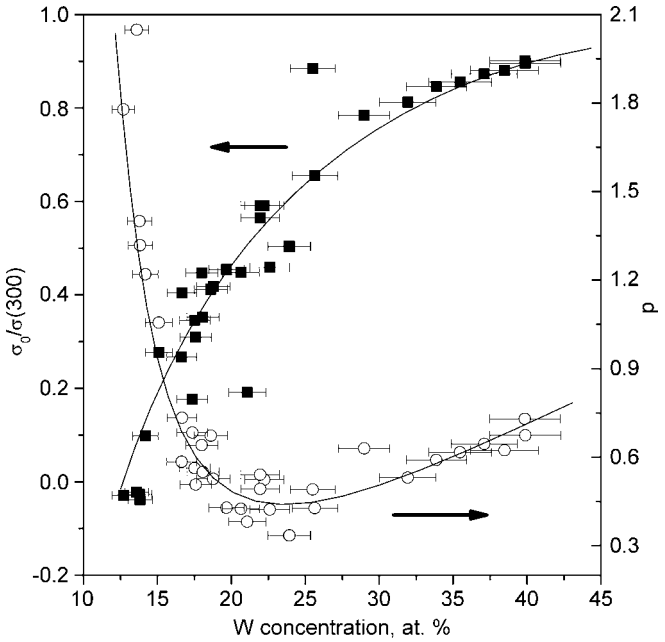

Figure 5. Dependence of the fitting parameters $\sigma_0/\sigma 300$, and p on tungsten concentration in the amorphous carbon–silicon nanocomposite films, containing W. Lines are guides to the eyes.

with the experimental conductivity–temperature dependence in Fe-containing SiO_2 films was found.

The model of inelastic tunnelling of electrons through a layer of amorphous insulator [16, 17] was used for the interpretation of the power-law dependences ($0 < p < 1.5$) of the conductivity on the temperature in granular (Co-Nb-Ta)-SiO_2 films in the wide range of metal concentration from 22.5 to 63 at.% [15].

In order to identify the mechanism of electron transport in the investigated films of W-containing amorphous carbon–silicon diamond-like nanocomposites, the fitting of $\sigma(T)$ curves was performed using both expressions (1) and (2). The expression (1) was taken with power exponent $m = 1/2$. The value of p in expression (2) was defined by fitting. As it was found, the best fitting of all sets of experimental $\sigma(T)$ dependences over the entire tungsten concentration range can be obtained using only the power-law dependence (2). The results of the fitting are shown in figure 2 by the solid lines as already mentioned above. It appeared that fitting parameters are strongly dependent on the value of tungsten concentration. In figure 5 these dependences of the power exponent p, and the normalized temperature-independent term $\sigma_0/\sigma(300)$ are shown.

The two regions of different p behaviour can be distinguished from an analysis of figure 5. At the lowest values of tungsten concentration studied, the decrease of p from 2.0 to 0.4 is observed as W concentration increases up to 23–25 at.%. For a further increase in tungsten concentration the growth of p from 0.4 to 0.7 takes place.

The behaviour of temperature-independent normalized conductivity $\sigma_0/\sigma(300)$ on W concentration is characterized by a monotonic increase with increase in metal concentration. The negative values of $\sigma_0/\sigma(300)$ are observed at the values of tungsten concentration less than 15 at.%. The pronounced growth of normalized conductivity in the temperature-independent

channel starts from the values of tungsten concentration more than 15 at.%. Although $\sigma_0 > 0$ in this W concentration range, the extrapolation of the conductivity to $T = 0$, performed at relatively high temperatures, does not allow us to identify with confidence the films as metallic ones. It is also necessary to point out that there are no peculiarities in the $\sigma_0/\sigma(300)$ curves for 23–25 at.% of W, where the minimum on tungsten concentration dependence of p is observed.

The temperature behaviour of the conductivity and the evolution of the fitting parameters with variation in tungsten concentration can be considered in terms of the model of inelastic tunnelling of electrons in thin films of amorphous dielectrics developed in [16, 17]. According to this model, the electron transport across a thin dielectric layer has a tunnelling character only at very low temperatures. With increase in temperature, it is replaced by the inelastic tunnelling of electrons through the pairs of localized states. With further increase in temperature, the inelastic conducting channels containing more localized states start to dominate. The temperature dependence of the average conductance due to the contribution of the conducting chains, containing n ($n > 1$) localized states, follows the power-law expression

$$\langle\sigma_n\rangle \sim Se^2\left(\frac{\Lambda^2}{\rho c^5}\right)^{(n-1)/(n+1)} g^n n^{2n} r_{loc}^{2n-1} d^{n-1} E_0^{2n/(n+1)} T^{n-[2/(n+1)]} \exp\left(-\frac{2d}{r_{loc}(n+1)}\right), \quad (3)$$

where e is the electronic charge, d is the distance between the electrodes, S is the cross-section area of the sample, Λ is the deformation potential constant, ρ is the density of dielectric, c is the velocity of sound in the dielectric, g is the density of localized states at the Fermi level, r_{loc} is the radius of the localized state and E_0 is the depth of localized states.

The fluctuations of the conductance of a sample are averaged if the number of conducting channels N containing n impurities will be sufficiently large, $N \gg 1$. This can take place in the case of large-area electrodes. In metal–insulator nanocomposite films, where the inelastic tunnelling occurs between the separate metal grains or clusters composed from the grains the effective area of electrodes should be taken into account, because of the existence of a large number of approximately equivalent conducting channels due to the complicated structure of the metal phase.

Following [16], the average conductance of the dielectric film is given by the sum of conductivities in all conducting channels:

$$\langle\sigma\rangle = \sum\langle\sigma_n\rangle. \quad (4)$$

In the temperature interval

$$T_n < T < T_{n+1}, \quad (5)$$

the highest contribution to the sum (4) is given by the term $\langle\sigma_n\rangle$. Other terms give only small corrections to (4) if $n < (d/a)^{1/3}$. The value of boundary temperature T_n is given by the expression [16]

$$T_n \sim (gr_{loc}^2 dn^2)^{-1}\left[\frac{\rho c^5}{\Lambda^2 E_0} gr_{loc}^2 d \exp\left(-\frac{d}{r_{loc}}\right)\right]^{2/(n^2+n+2)}. \quad (6)$$

In the case of metal–carbon composites, where the carbon insulating phase is characterized by essential structural non-homogeneities, the inelastic conducting channels with a different number of localized states may contribute to the total conductance simultaneously.

Applying this model to the description of electron transport in the investigated W-containing carbon–silicon nanocomposite films, it is possible to calculate the average number

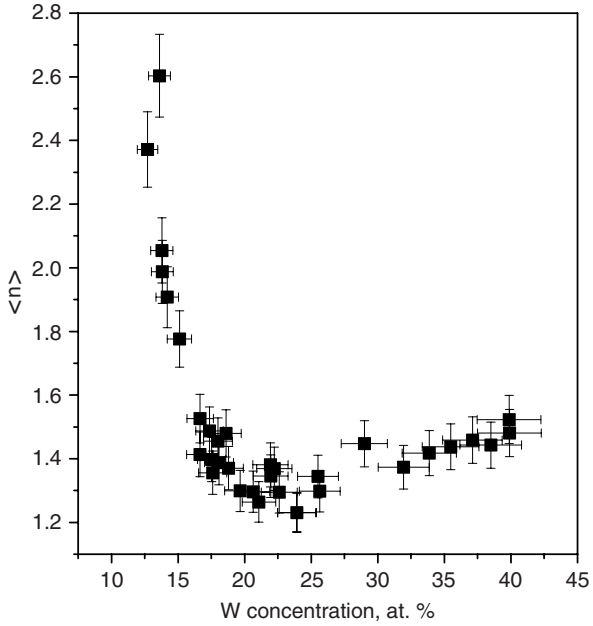

Figure 6. Dependence of the average number $\langle n \rangle$ of the localized states in the intercluster potential barriers as a function of tungsten concentration in W-containing amorphous carbon–silicon nanocomposite films. Explanations are given in the text.

$\langle n \rangle$ of localized states in the conducting channels between metal clusters from (3):

$$\langle n \rangle = \tfrac{1}{2}(p - 1 + (p^2 + 2p + 9)^{1/2}), \tag{7}$$

where p is the power exponent in expression (2). The results of this calculation are presented in figure 6, where the dependence of the average number of localized states $\langle n \rangle$ is shown as a function of tungsten concentration. As one can see from figure 6, the dependence of $\langle n \rangle$ on the metal concentration is non-monotonic in W-containing amorphous carbon–silicon nanocomposite films. Qualitatively, it is similar to the concentration dependence of the power exponent p presented in figure 5 and discussed above.

The initial decrease of $\langle n \rangle$ from 2.6 to 1.3 observed at W concentration range less than 23–25 at.% occurs due to the decrease in the distance between tungsten clusters due to an increase in metal concentration. The increase of $\langle n \rangle$ from 1.3 to 1.5 observed at high W concentration may be ascribed essentially to the enhanced intercluster defect generation caused by the structural transformation of the host matrix.

In the range of tungsten concentration exceeding 15 at.%, starting from which the value of the temperature-independent term $\sigma_0/\sigma(300)$ is positive, the tunnel junctions with no or one localized state form an infinite cluster. This infinite cluster is partly shunted by the separate tunnel junctions or the chains of serially connected tunnel junctions with a wide-ranged number of localized states in the intercluster potential barriers. These junctions or the chains of junctions are responsible for the temperature-dependent term of the conductivity of the nanocomposite films studied.

The inelastic tunnelling model being applied to the description of the electron transport in metal–dielectric nanocomposites below the metal–insulator transition does not take into

account the grain charging energy. It is estimated as $E_C \approx e^2/D\kappa$, where κ is the effective dielectric constant of the medium [10], and is equal to the energy necessary to generate a charge carrier on a single metal grain. Thus the applicability of the model is limited by temperature $T \gg E_C$, and metal concentration range close to the percolation threshold value, where the tunnelling between metal clusters composed from the separate metal grains will dominate [27]. Far in the dielectric region, when $n \to \infty$ the transition to hopping conductivity (1) with $m < 1$ will occur.

Above the percolation threshold, the model ignores the effect of the infinite conducting cluster, consisting of the mechanically connected metal grains, on the electron transport. Only the conduction in the tunnel junctions between metal clusters, and the chains of such junctions, which shunt the infinite conducting cluster, is taken into account.

The model separates the tunnel junctions in different groups, each one characterized by a certain number of the localized states in the potential barriers between metal clusters. The different types of tunnel junctions give different contribution to the temperature dependence of the conductivity of tungsten–carbon nanocomposite films according to (3). The evolution of the infinite conducting cluster structure by an increase in metal concentration can be related to the multicomponent or 'polychromatic' percolation originally introduced in [29].

The evolution of Raman spectra of W-containing carbon–silicon diamond-like nanocomposite films with increase in tungsten concentration correlates with the above-discussed evolution of the fitting parameters of conductivity. The dependences of the fitting parameters of Raman spectra on tungsten concentration—G peak position shift and on the intensity ratio of $I(\mathrm{D})/I(\mathrm{G})$ peaks obtained by the fitting of the initial Raman spectra (figure 3) and shown in figure 4 confirm the effect of the modification of carbon phase structure on the conductivity. As can be seen from figure 4, both dependences demonstrate a similar behaviour. When W concentration is in the range $\lesssim$ 21–22 at.%, the position of the G peak and intensity ratio of $I(\mathrm{D})/I(\mathrm{G})$ peaks does not depend on it. For a further increase in W concentration a sharp transition-like growth of both parameters is observed: the upshift of G peak from 1500 to 1530 cm^{-1} takes place and the intensity ratio of $I(\mathrm{D})/I(\mathrm{G})$ peaks increases from 0.9 to 2.0. It is necessary to note that the sharp increase of both parameters starts at the same value of the tungsten concentration, where the growth of p was found to take place.

The Raman spectra of carbon and carbon-based materials depends mainly on the macrostructure of the carbon phase determined in turn by the existence of sp^2 rings or chains, and bond-angle disorder [21]. Clustering of sp^2 sites leads to an increase in the intensity ratio of $I(\mathrm{D})/I(\mathrm{G})$ peaks. As shown in [21, 22], in highly disordered amorphous carbons, if the characteristic Raman peaks' width exceeds 50 cm^{-1}, the value of $I(\mathrm{D})/I(\mathrm{G})$ ratio is proportional to the in-plane correlation length L_a or sp^2 coordinated carbon cluster size in the range below 2 nm as

$$\frac{I(\mathrm{D})}{I(\mathrm{G})} = CL_a^2, \tag{8}$$

where $C \approx 0.0055$ for the excitation wavelength 514 nm. Taking into account the dispersion of the Raman spectra with excitation wavelength [24, 25], the observed increase of $I(\mathrm{D})/I(\mathrm{G})$ ratio from 0.9 to 2.0 corresponds to the increase of the sp^2 cluster size approximately from 0.7–0.9 to 1.2–1.4 nm.

The upshift of G peak confirms enhanced sp^2 clustering [21]. This structural reorganization of the carbon phase in carbon–silicon host matrix can occur due to the ability of sp^2 clusters diffuse within matrix and to coalescence into the large aromatic clusters [22]. Assuming that the increase in the average number of the localized states in the potential barriers between metal clusters correlates well with the increase in sp^2 cluster size, it is possible to associate

the localized states with these graphitic clusters. Despite that the band gap of such clusters, depedent on the number of aromatic rings [24], is rather wide, the defect states at their grain boundaries [28] or defects in clusters with an odd number of sp^2 sites [24] can participate in the electron tunnelling. The observed joint evolution of the carbon-phase structure and the conductivity of tungsten-containing carbon–silicon nanocomposite films supports the proposed model regarding the principal influence of the properties of the potential barriers between metal clusters on the electron transport in the investigated films over the temperature range 80–400 K.

The increase in tungsten concentration in the films studied is accompanied by the increase in intensity of the bombardment of the growing surface of the films by sputtered W atoms. This can lead to a growth of the substrate temperature during deposition. As was shown in [22], the increase in the deposition temperature of ta-C films up to 200 °C was responsible for the coalescence of sp^2 sites in the planar graphitic clusters. The increase in concentration of sp^2 sites was not observed up to this temperature.

Furthermore, the low-energy bombardment of the surface of the growing film by tungsten atoms may enhance the diffusion of sp^2 sites and decrease the characteristic temperatures for the above processes of structural reorganization of the carbon phase. This is in contrast with the results of [26], where the increasing fluence of post-deposition implantation of W ions caused the enhancement of disorder in hydrogenated amorphous carbon films.

4. Conclusion

The evolution of the electron transport mechanisms in tungsten-containing amorphous carbon–silicon diamond-like nanocomposite films with increase in tungsten concentration (12–40 at.%) was studied in the temperature interval 80–400 K.

It was shown that the temperature dependences of the conductivity over the entire range of temperature and tungsten concentration are well fitted by the power-law dependence. The parameters of the fitting are functions of the tungsten concentration.

The main conduction mechanism in the investigated films is well described in the framework of the model of inelastic tunnelling of the electrons between the tungsten clusters dispersed in the insulating carbon–silicon matrix. The existence of the localized states in the intercluster barriers in carbon–silicon matrix enhances the transparency of the barriers and reduces the temperature dependence of the conductivity.

At tungsten concentration less than 23–25 at.% the decrease in the average number of the localized states from 2.6 to 1.3 was found to take place. This process follows the decrease in the intercluster distances due to the tungsten-concentration enhancement.

Growth of the average number of localized states in the intercluster potential barriers from 1.3 to 1.5 observed at W concentration exceeding 23–25 at.% was explained as a result of the defect generation accompanied by the increase in W concentration. This was supported by the Raman spectra of the W-containing carbon–silicon nanocomposite films which are characterized by the expressed increase of $I(\mathrm{D})/I(\mathrm{G})$ ratio and G peak-position shift increase with metal concentration determined by the rearrangements of sp^2 carbon sites.

Acknowledgments

This work was in part supported by the Russian Foundation for Basic Research (grant no. 03-02-16655), and by Research Fellowships of the Japan Society for the Promotion of Science for Young Scientists.

References

[1] Gerstner E G, Lukins P B, McKenzie D R and McCulloch D G 1996 *Phys. Rev.* B **54** 14504
[2] Dimigen H, Hübsch H and Memming R 1987 *Appl. Phys. Lett.* **50** 1056
[3] Lutsev L V, Zvonareva T K and Lebedev V M 2001 *Tech. Phys. Lett.* **27** 659
[4] Huang Q F, Yoon S F, Rusli, Yang H, Gan B, Chew K and Ahn J 2000 *J. Appl. Phys.* **88** 4191
[5] Gouy-Pailler Ph and Pauleau Y 1993 *J. Vac. Sci. Technol.* A **11** 96
[6] Lutsev L V, Yakovlev S V and Siklitskii V I 2000 *Solid State Phys.* **42** 1139
[7] Dorfman B F 1998 *Thin Solid Films* **330** 76
[8] Dorfman V 1992 *Thin Solid Films* **212** 267
[9] Dorfman V F and Pypkin B N 1991 *Surf. Coat. Technol.* **48** 103
[10] Sheng P, Abeles B and Arie Y 1973 *Phys. Rev. Lett.* **31** 44
[11] Meilikhov E Z 1999 *Sov. Phys.—JETP* **88** 819
[12] Zakheim D A, Rozhansky I V, Smirnova I P and Gurevich S A 2000 *Sov. Phys.—JETP* **91** 553
[13] Boghosian H H and Howson M A 1990 *Phys. Rev.* B **41** 7391
[14] Carl A, Dumpich G and Wasserman E F 1994 *Phys. Rev.* B **50** 4802
[15] Lutsev L V, Kalinin Yu E, Sitnikov A V and Stognei O V 2002 *Phys. Solid State* **44** 1889
[16] Glazman L I and Matveev K A 1988 *Sov. Phys.—JETP* **67** 1276
[17] Glazman L I and Shekhter R I 1988 *Sov. Phys.—JETP* **67** 1462
[18] Meilikhov E Z 2001 *Sov. Phys.—JETP* **93** 625
[19] Aronzon B A, Varfolomeev A E, Kovalev D Yu, Likhalter A A, Ryl'kov V V and Sedova M A 1999 *Phys. Solid State* **41** 857
[20] Teplinskii V M, Gantmakher V F and Barkalov O I 1992 *Sov. Phys.—JETP* **74** 905
[21] Ferrari A C and Robertson J 2000 *Phys. Rev.* B **61** 14095
[22] Chhowalla M, Ferrari A C, Robertson J and Amaratunga G A J 2000 *Appl. Phys. Lett.* **76** 1419
[23] Altshuler B G and Aronov A G 1983 *JETP Lett.* **37** 410
[24] Robertson J 2002 *Mater. Sci. Eng.* **R37** 129–281
[25] Shi J R, Shi X, Sun Z, Lau S P, Tay B K and Tan H S 2001 *Diamond Relat. Mater.* **10** 76–81
[26] Konchits A A, Valakh M Ya, Shanina B D, Kolesnik S P, Ivanchuk I B, Carey J D and Silva S R P 2003 *J. Appl. Phys.* **93** 5905–10
[27] Laibowitz R B, Alessandrini E I and Deutscher G 1982 *Phys. Rev.* B **25** 2965
[28] Dasgupta D, Demichelis F and Tagliaferro A 1991 *Phil. Mag.* B **63** 1255
[29] Zallen R 1977 *Phys. Rev.* B **16** 1426–35